

MECHANICAL BEHAVIOR AND SWELLING OF TUBE SCALE FROM A PRESSURIZED WATER REACTOR STEAM GENERATOR USING MINIATURE SPECIMENS

M.P. MANAHAN, Sr.

Battelle Columbus Division, 505 King Avenue, Columbus, OH 43201-2693, USA

Received 27 July 1988; accepted 11 January 1989

Flakes consisting primarily of iron oxide (magnetite) have been discovered in the spaces between tubes and support plates in steam generators, increasing flow resistance and causing abnormal increases in water levels. To determine the effects of tube scale on steam generators and to study the fracture and swelling behavior of the flakes, this investigation measured the elastic modulus, fracture stress, and swelling of scale from the steam generator of the Oconee-2 pressurized water reactor (PWR). Evidence indicates that the mechanical behavior response of the flakes is quite complex. The flakes are composed of multiple layers, each of which exhibits a different mechanical behavior. The fracture stress of the strongest flake materials tested was in the range of 117 to 165 MPa (17 to 24 ksi). Thin, single-layered specimens exhibited moduli in the range of 137 880 to 227 502 MPa (20 to 33×10^6 psi) and layered specimens from 48 258 to 86 175 MPa (7.0 to 12.5×10^6 psi) at room temperature. There does not appear to be a substantial change in the range of stresses measured at elevated temperatures.

1. Introduction

Tube scale that consists primarily of iron oxide (magnetite) may lodge in the spaces between the tubes and support plates in steam generators, increase flow resistance, and cause abnormal increases in steam generator water levels. The hydrodynamic (water slap) process for cleaning scale from the tubes can be enhanced through preconditioning the scale by, for example, pre-wetting, predrying, or thermal cycling. Better understanding of the mechanical properties of the scale will permit more effective hydrodynamic cleaning. Battelle used its patented miniature specimen technique* to measure important specimen properties such as elastic modulus, fracture stress, and swelling [1]. The Electric Power Research Institute (EPRI) has published earlier work on specimens with an oxide layer attached to a relatively thick substrate [2], but to the best of the author's knowledge, the present study is the first attempt to measure bulk properties of the thin flakes themselves. Studies of the thermal expansion, thermal conductivity, and curling behavior of the Oconee-2 flake specimens are reported by Manahan [3].

2. Metallography and specimen preparation

2.1. Metallography

Sludge from the generator was sorted and the largest flakes were removed for metallographic investigation and specimen preparation. Metallographic studies were conducted to determine the microstructure of the flakes, and to determine if anisotropy occurs in the plane normal to the tube radius. The flakes were found to be reasonably isotropic. Photomicrographs were made both before (as-polished) and after etching. The average grain size near the center of the cross section was determined to be 0.005 mm (0.2 mils), as shown in figs. 1 and 2. Near the outside diameter (OD) surface, grains as large as 0.01 mm (0.5 mils) were observed. Hence, a minimum specimen dimension of about 0.1 mm (5.0 mils) is required for continuum behavior. The majority of flakes tested met the continuum thickness requirement.

An important difference was observed between the surface morphologies of the flake inside diameter (ID) and OD surfaces. The ID surfaces were noticeably smoother, with linear striations oriented in the circumferential direction of the tubes. The OD surfaces were rougher and porous in appearance. Photomicrographs of the flake cross section confirmed that the outer surfaces showed appreciable porosity (see fig. 2).

* The techniques described are explained in part in US Patent No. 4567774 dated February 4, 1986.

The etchant used was 45% H₂O, 30% HCl, 20% HNO₃ and 5% HF.

There appear to be three groupings of grain size for the flake shown in fig. 2. The small grains are located near the ID surface and extended through approximately one-third the thickness of the flake. The intermediate size grains are located in the central portion of the cross section and extend over a distance of approximately one-half of the specimen thickness. The largest size grains are located in the porous region near the tube OD surface. The number and thickness of the regions vary widely from flake to flake.

A photomicrograph of a flake sectioned parallel to the tube axis in the as-polished condition is shown in fig. 3. Copper-colored particles were observed in the material. Further work is needed to determine the particle compositions.

2.2. Specimen preparation

The sorted flakes were found to be irregular in shape with typical dimensions in the axial direction (i.e., parallel to the tube axis) of 3.81 and 5.08 mm (0.15 to 0.20 inch), along the circumferential direction of about 2.54 mm (0.10 inch), and from 0.1 to 0.2 mm (4.0 to 8.0 mils) in thickness.

For the determination of elastic modulus and fracture stress, flakes were machined into curved beams that were tested in a four-point bend fixture. For tests of

swelling, flakes were machined into thin, straight beams. The bend specimens were machined so that their length dimension was parallel to the hoop direction of the Inconel tubes, while the swelling specimens were oriented so that their length was parallel to the tube axis.

As a consequence of the dimensions of the flake samples received, the length of the bend test specimens was nominally 2.54 mm (0.10 inch), while the swelling specimens were up to 5.08 mm (0.20 inch) long. The bend specimens were machined to a nominal width of 1.91 mm (0.075 inch), and the swelling specimens had a nominal width of 1.27 mm (0.050 inch).

3. Test methods and results

3.1. Elastic modulus and fracture stress

A four-point static bend test measured the modulus and fracture stress. For a brittle material such as magnetite, four-point bend loading is preferable to three-point loading. A brittle specimen in a three-point bend test may not fracture at the point of maximum bending moment, i.e., at the point of load application. However, in a four-point bend test, the entire region between the two loading points is at a constant maximum value of bending moment. Provided the test specimen fractures between the two load points, a constant value of maxi-

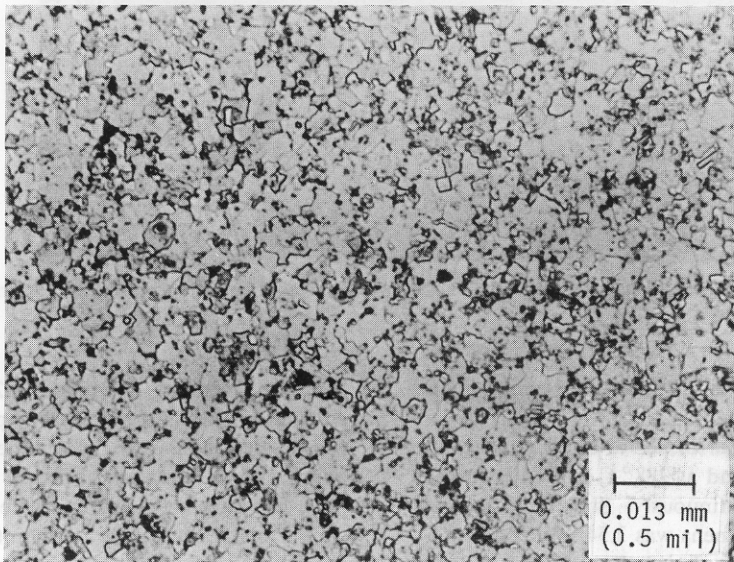


Fig. 1. Microstructure of magnetite flake near center of cross section.

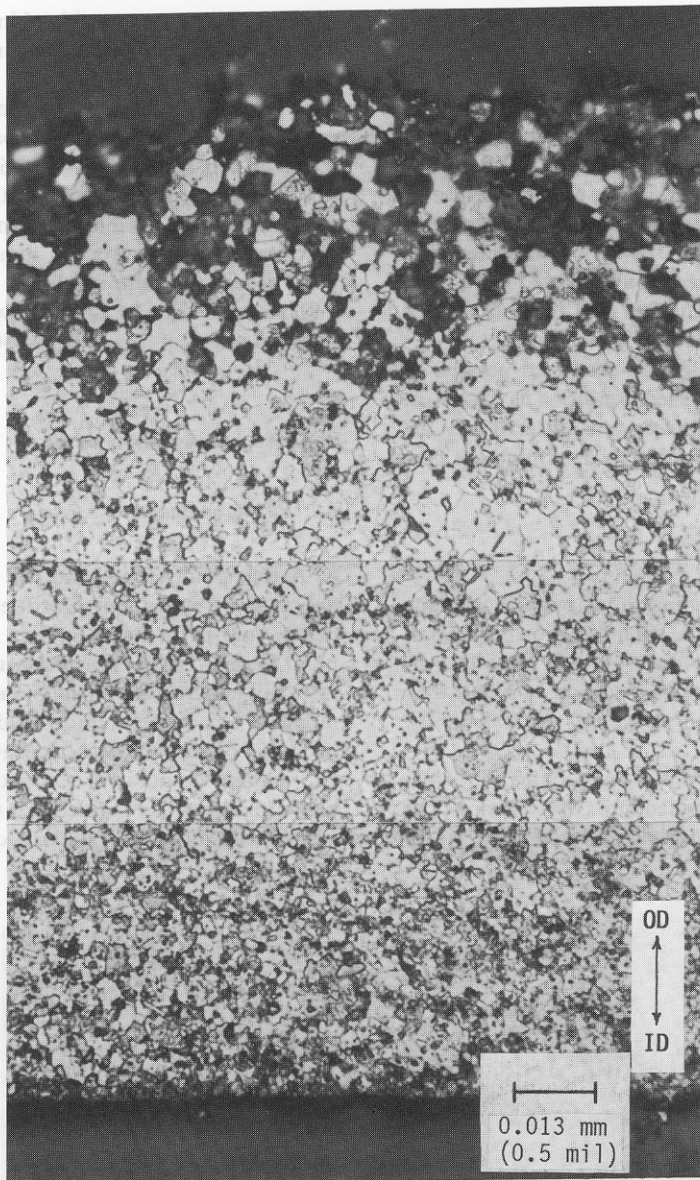


Fig. 2. Photomontage of magnetite flake, showing increased porosity toward the OD surface.

imum bending moment may be used in the equations for fracture strength and modulus.

The bend tests were performed at room temperature [RT, or 20°C (68°F)] and at 288°C (550°F), and the load was increased continuously. Since the nominal length of the bend specimens was 2.54 mm (0.10 inch), the specimen support was designed to allow a distance of 2.03 mm (0.08 inch) between supports, giving the test

beam an overhang of at least 0.25 mm (0.01 inch) on either side of the support. A one-piece specimen loading punch, designed with twin blades 1.0 mm (0.04 inch) apart, slid in grooves machined in the specimen support. Because the specimens were small and the dimensional tolerances had to be maintained at the test temperature, the specimen support and loading punch were machined from Invar.

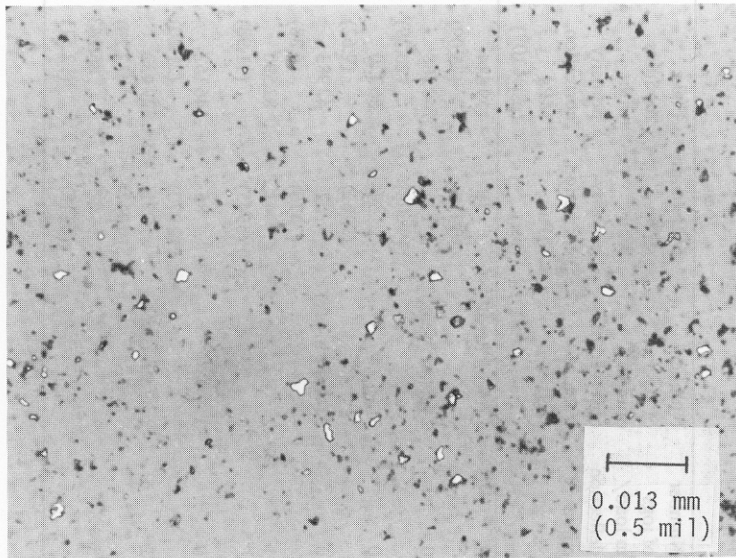


Fig. 3. Magnetite in the as-polished condition sectioned parallel to the tube axis. White areas are copper-colored particles.

Fig. 4 shows a schematic drawing of the loading apparatus. The specimen's support block rests on a heated stage that can be moved in the x - y direction by micrometer drives. The load arm is pressed against the specimen punch by a pneumatic actuator, and this load

is reacted through a precision load cell. The rate of load application is determined using an adjustable leak in the pneumatic system, actuated by opening and closing an exhaust valve. The bend test used a rate of load application of approximately 4.7 kg/min (10.4 lb/min).

Table 1
Benchmark data for miniature four-point bend test performed on porcelain specimens

Specimen identification	Miniature Specimens		Large Specimens	
	Maximum stress, MPa (psi)	Elastic modulus, MPa ($\times 10^6$ psi) (bending)	Maximum stress (psi)	Elastic modulus, MPa ($\times 10^6$ psi)
PORC 1	51 (7340)	47086 (6.83)	-	-
PORC 2	42 (6125)	46190 (6.70)	-	-
PORC 6	56 (8116)	58944 (8.55)	-	-
PORC 8	47 (6802)	50877 (7.38)	-	-
PORC 10	38 (5469)	41639 (6.04)	-	-
Average	47 (6770)	48947 (7.10)	72 (10514) (bend)	71008 (10.3) (uniaxial compression) 73076 (10.6) (pulse/echo)

Table 2
Mechanical behavior of flakes at room temperature, 20 °C (68 °F)

Specimen identification	Orientation	Condition	Maximum stress, MPa (psi)	Flake modulus, MPa (psi × 10 ⁶)	Specimen thickness, mm (inch × 10 ⁻³)	Maximum load, kg (lb)	Number of jogs in load/deflection curve	Number of layers optically observed in fracture surface	Maximum stress with porosity correction, MPa (psi)	Flake modulus with porosity correction, MPa (psi × 10 ⁶)
M2UD	Concave up	Dry	73 (10577)	186758 (27.09)	0.101 (3.99)	0.094 (0.207)	0	1 (clean break)	71 (10316)	179684 (26.09)
M1UD	Concave up	Dry	69 (10066)	51705 ^{a)} (7.50)	0.116 (4.55)	0.111 (0.245)	0	2 (clean break)	135 (19608)	140568 (20.39)
M10UW	Concave up	Wet	61 (8799)	80039 (11.61)	0.137 (5.41)	0.142 (0.313)	0	3	54 (7762)	66320 (9.62)
M12UW	Concave up	Wet	50 (7310)	42535 (6.17)	0.181 (7.14)	0.213 (0.470)	0	1 (clean break)	52 (7476)	43983 (6.38)
M8UD	Concave up	Dry	27 (3967)	45017 (6.53)	0.198 (7.81)	0.133 (0.293)	1	2	41 (5945)	82590 (11.98)
M3DD	Concave down	Dry	77 (11117)	126022 (18.28)	0.137 (5.40)	0.131 (0.289)	0	3	85 (12270)	146152 (21.20)
M5DW	Concave down	Wet	88 (12806)	126573 (18.36)	0.151 (5.95)	0.169 (0.373)	2	2 (clean break)	131 (19037)	229432 (33.28)
M13DD	Concave down	Dry	29 (4221)	49429 (7.17)	0.201 (7.91)	0.105 (0.231)	3	3	42 (6118)	86243 (12.51)

^{a)} First test to define load/displacement range. Modulus is approximate due to non-linear compliance.

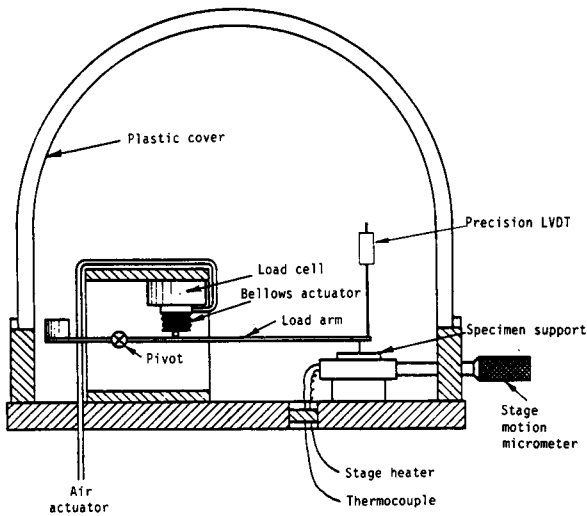


Fig. 4. Schematic drawing of the bend test apparatus.

The exact value of bending moment at the point of fracture must be known to evaluate the fracture strength of the material from flexure equations. The four-point bend stress/strain relationships are provided in the literature [4–6]. Since the beams are initially curved, the flat plate solution was compared with the curved beam solutions using both the hyperbolic stress distribution

approximation and the exact solution for an initially curved beam in pure bending. Since the difference between the flat plate and curved beam solutions is small for the geometry of interest ($\sim 1\%$), the flat plate equations were used to analyze the data. In all tests, the load train compliance was measured [RT, 288°C (550°F)] and the data were adjusted for compliance. The specimen preload (dead weight of the punch) was added to the recorded data. The measured punch, support, and specimen dimensions after machining were used in the calculations.

Benchmark bend test data porcelain specimens machined to approximately the same dimensions as the flakes were compared with large specimen data. The miniature and large specimen data are compared in table 1. The average miniature bend modulus is approximately 30% lower than the average large specimen modulus determined in compression. This difference is probably due to the measurement technique (bending versus compression) and the uncertainty in the specimen thickness in the vicinity of the crack. The difference in the fracture stress is probably due to specimen thickness uncertainties, as well as the effects of surface scratches on the miniature specimens. Although the specimens were polished, small scratches on the miniature specimens are likely to have a greater effect on fracture stress than in large specimens.

Table 3
Mechanical behavior of flakes at room temperature corrected for specimen thickness

Specimen ID	Layer 1 (ID surface) thickness, mm (mils)	Layer 2 thickness, mm (mils)	Porous layer (OD surface) thickness, mm (mils)	Comments	Maximum stress with specimen thickness correction, MPa (psi)
M2UD	0.103 (4.04)	–	Not measurable	Clean break	71 (10316)
M1UD	0.0828 (3.26)	–	0.021 (0.84)	Clean break	135 (19608)
M10UW	~ 0.11 (~ 4.30)	~ 0.0371 (~ 1.46)	~ 0.016 (~ 0.64)	ID/OD surfaces not parallel; striations covered by black material	96 (13928)
M12UW	0.179 (7.06)	–	Not measurable	Clean break; rough OD surface	52 (7476)
M8UD	0.0815 (3.21)	0.0805 (3.17)	0.012 (0.47)	No evidence of striations	162 (23483)
M3DD	0.020 (0.78)	0.111 (4.36)	0.014 (0.54)	Faint evidence of striations	118 (17053)
M5DW	0.124 (4.88)	–	0.0262 (1.03)	Clean break; striation partly covered; OD layer rough	131 (19037)
M13DD	0.103 (4.05)	0.0640 (2.52)	0.0361 (1.42)	OD layer very rough; almost no evidence of striations on ID surface	111 (16101)

Table 4
Mechanical behavior of flakes at 288 °C (550 °F)

Specimen identifi- cation	Orientation	Condition	Maximum stress, MPa (psi)	Flake modulus, MPa (psi × 10 ⁶)	Specimen thickness, nm (inch × 10 ⁻³)	Maximum load, kg (lb)	Number of jogs in load/ deflection curve	Number of layers optically observed in fracture surface	Maximum stress with porosity correction, MPa (psi)	Flake modulus with porosity correction MPa (psi × 10 ⁶)
M4DT	Concave down	Dry	95 (13804)	65286 (9.47)	0.113 (4.46)	0.106 (0.234)	1	1	117 (16907)	88518 (12.84)
M7UT	Concave up	Dry	96 (13941)	166765 (24.19)	0.116 (4.57)	0.116 (0.366)	0	1	97 (14064)	168971 (24.51)
M9UT	Concave up	Dry	70 (10181)	125746 (18.24)	0.127 (4.99)	0.140 (0.309)	1	1	52 (7509)	79694 (11.56)

Table 5
Mechanical behavior of flakes at 288°C (550°F) corrected for specimen thickness

Specimen ID	Layer 1 (ID surface) thickness, mm (mils)	Layer 2 (OD surface) thickness, mm (inch)	Porous layer thickness, mm (inch)	Comments	Maximum stress with specimen thickness correction, MPa (psi)
M4DT	0.102 (4.03)	–	Not measurable	Broke into 4 pieces	117 (16907)
M7UT	0.116 (4.55)	–	Not measurable	Broke into 3 pieces	97 (14064)
M9UT	0.148 (5.81)	–	Not measurable	Broke into 4 pieces	52 (7509)

The miniature flake data are presented in tables 2 through 5 for the room temperature (RT) and 288°C (550°F) tests, respectively. Specimens are identified by a four-character alphanumeric sequence. The first character, “M,” indicates magnetite flakes. The second character is an arbitrary sequential number. The third character indicates whether the specimen was tested concave up (“U”) or concave down (“D”). The last character indicates whether the specimen was tested wet (“W”) at RT, dry (“D”) at RT, or dry at 288°C (“T”).

Flake response under loading is very complex. Jogs in the load/deflection curve were observed for several of the specimens. The apparatus was checked and found to be performing properly, with no slippage in the load train. Visual examination of the fracture surface showed that the crack did not propagate straight through the thickness for all specimens. As shown in fig. 5, some specimens exhibited fracture within the bulk material during testing, which resulted in a layered specimen. The crack plane was oriented in the hoop direction, which would explain the loss of stiffness that may have resulted in jogs in the load/deflection curve. However, not all specimens that were layered after testing had jogs in the load/deflection curve.

After testing, it was observed that portions of striations on the ID surface of several specimens were covered with a material that is similar to the OD surface material (fig. 6). This may be relevant to the study of scale formation and transport. If the striations are an artifact of the tube machining revealing from flakes spalling off the tube, then the material found on the ID surface may have been deposited there after the flake was removed from the tube. Alternatively, the material could have attached during contact with the OD surface of other flakes (i.e., residual magnetism or chemical bonding).

Another explanation for the loss of stiffness during some tests is partial through-thickness cracking. However, this is an unlikely explanation, because calculations indicate that cracking of the layers would result in stresses high enough to crack the remaining ligament. In future experiments, after a jog in the curve is observed, it would be helpful to stop the test, section the specimens, determine if a crack is present in the material, and observe the orientation of the crack (hoop or through-thickness).

As mentioned earlier, the metallographic analysis supports the explanation of internal hoop oriented cracking. Fig. 2 shows three groupings of grain size that change fairly abruptly through the thickness. From a mechanical behavior viewpoint, it is as if there are three different materials laminated together. In addition, Hairston and Frye reported chemical variations through the thickness of some flakes [7]. As stated by Szlarska-Smialowska, magnetite has been observed to form in layers and/or have a chemical gradient through the thickness [8]. Individual materials in the layers could be studied by separating the layers after testing. Useful tests would include chemical analysis, X-ray diffraction, and metallography.

As a result of these observations, it is not possible to report an elastic modulus in the conventional sense. The elastic modulus is a measure of the displacement of atoms from their equilibrium positions in a given material. Since a given flake may have compositional variation through the thickness and varying grain size (indicating different mechanical response within each layer), a “flake modulus” is reported that is calculated based on the initial slope of the load deflection curve. As a result of these considerations, large variations in the flake modulus are to be expected as shown in tables 2 through 5. As shown in tables 3 and 5, the layer

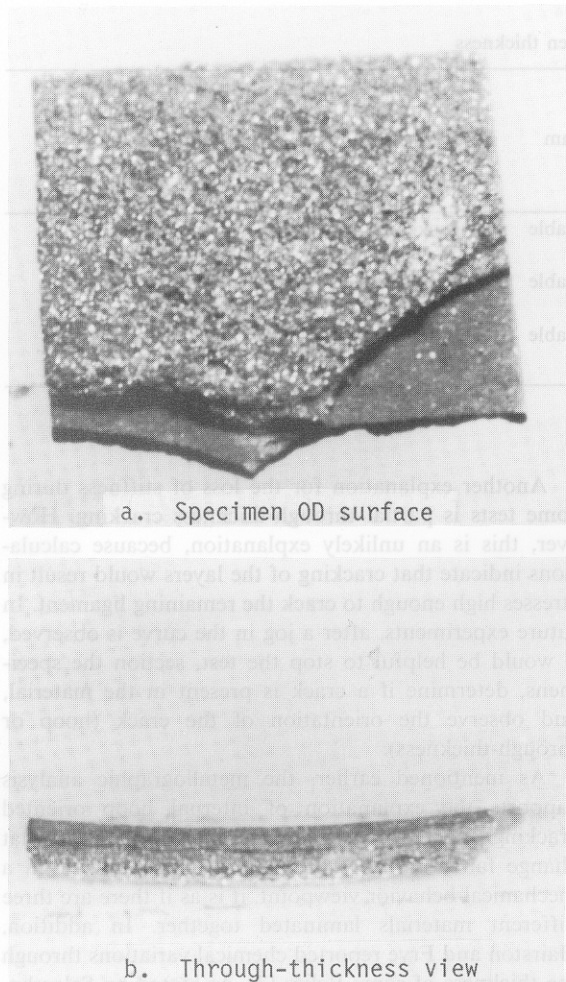


Fig. 5. Fracture surface of a magnetite flake specimen (M13DD) showing a layered fracture appearance.

thicknesses were measured at the fracture surfaces of each specimen and the results based on the nominal pretest thickness measurements were corrected.

The high level of porosity in the OD surface layer indicates that this layer has negligible load carrying capacity. Therefore, in tables 2 and 4, the stresses and flake moduli were recalculated by using the specimen thickness at fracture and subtracting the thickness of the porous layer from the overall specimen thickness. After this data correction, there is a distinct trend in the data of a decrease in flake modulus with increasing

thickness. The thin single-layered specimens tested at RT exhibit moduli [140569 to 229432 MPa (20.39 to 33.28×10^6 psi)] that are comparable to handbook data for magnetite [227502 MPa (33.0×10^6 psi)].

In tables 3 and 5, a further correction was applied to the fracture stress data. It is postulated that, prior to testing, the layers are continuous and, at a certain load, the layers separate in the central portion of the flakes. Although the stress field in the layered specimens is fairly complex, a simple correction can be applied to estimate the fracture stress in the material. The following corrections were made to the fracture stress data:

1. The actual thickness of the layers at the fracture surface was used in the stress calculation.
2. The porous layer does not carry any load.
3. For specimens containing two nonporous layers, only the thickest layer is used in the stress computation.

As shown in tables 3 and 5, these corrections bring the data into more consistent agreement. There appear to be two distinct materials present at room temperature: one with a fracture stress in the range of 117 to 165 MPa (17 to 24 ksi) for specimens of thickness 0.08 to 0.12 mm (3.2 to 4.8 mils); the second with a fracture stress in the range of 51.7 to 110.3 MPa (7.5 to 16.0 ksi) for specimens of thickness 0.10 to 0.18 mm (4.0 to 7.0 mils). A similar trend is observed for the high temperature tests.

3.2. Swelling

A Sheffield Accutron Model 50185 vertical comparator was used for the swelling measurements, which were

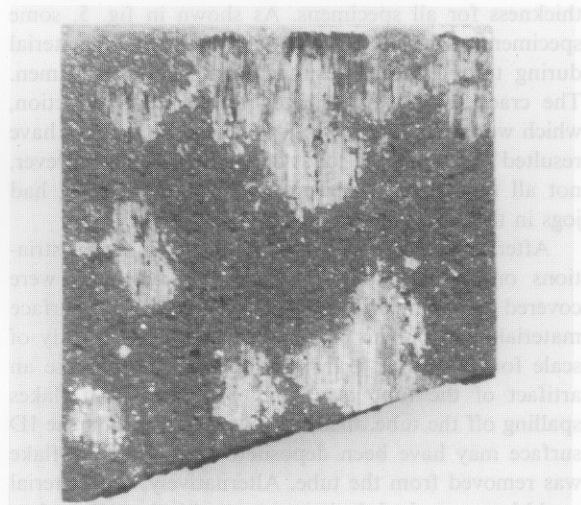


Fig. 6. ID surface of a magnetite flake specimen (M10UW) wet tested at room temperature.

made in a temperature- and humidity-controlled laboratory. The system is capable of length measurement with an uncertainty of $\pm 12.7 \times 10^{-6}$ mm ($\pm 0.5 \times 10^{-3}$ mils). The room temperature was carefully controlled to $20 \pm 0.6^\circ\text{C}$ ($68 \pm 1^\circ\text{F}$) and the relative humidity was 39.4%. Calibration runs were made prior to taking measurements on a specimen. The calibration runs were necessary to account for the shortening of the stylus after distilled water was added. Readings were taken every half-hour for several hours. After subtracting the calibration curve for each specimen, there was no detectable swelling in the flakes. Since the measurement uncertainty is $\pm 12.7 \times 10^{-6}$ mm ($\pm 0.5 \times 10^{-3}$ mils), any swelling may be presumed to be below 0.0017%.

4. Conclusions

The mechanical behavior response of the flakes is quite complex. Evidence suggests that the flakes are composed of two, or, for thicker flakes, three layers of material, each of which exhibits different mechanical properties. There does not appear to be any significant change in the mechanical behavior of the flakes when tested wet. However, the data are sparse and there is considerable scatter due to the nature of the flakes and the fact that they were tested in the as-received condition.

The fracture stress of the strongest flake materials tested was in the range of 117 to 165 MPa (17 to 24 ksi). There does not appear to be a substantial change in the range of stresses measured at elevated temperature. The thin, single-layered specimens tested at RT exhibited moduli of 137 880 to 227 502 MPa (20 to 33×10^6 psi). The layered specimens and single-layer specimens exhibited moduli in the range of 48 258 to 86 175 MPa (7.0 to 12.5×10^6 psi) at RT. The flake swelling was below

the measurement uncertainty. Therefore, the swelling, if it occurs, is below 0.0017%.

Acknowledgements

The author wishes to acknowledge Duke Power Company and MPR Associates, Inc., for their support of the work reported. Particular thanks for assistance and support are given to R. Eaker of Duke Power and to J. Nestell and N. Cole of MPR Associates. Special thanks also go to Battelle staff involved in the testing: N. Frey, C. Charles, D. Rider, and J. Parks.

References

- [1] M.P. Manahan, A.S. Argon and O.K. Harling, Determining mechanical behavior of solid materials using miniature specimens, US Patent Number 4567774, February 4, 1986.
- [2] J. Armitt, R. Holmes, M.I. Manning, D.B. Meadowcroft and E. Metcalfe, The Spalling of Steam-Grown Oxide from Superheater and Reheater Tube Steels, Report to EPRI from Central Electricity Research Laboratories (February 1978) pp. 3-1 to 3-14.
- [3] M.P. Manahan, Thermal Expansion and Conductivity of Magnetite Flakes Taken from the Oconee-2 Steam Generator (July 1988) in press.
- [4] F.L. Singer, in: Strength of Materials (Harper & Bros., New York, 1962) Art. 6.2.
- [5] F.R. Shanley, in: Strength of Materials (McGraw-Hill, New York, 1957) sec. 16.11.
- [6] S.P. Timoshenko and J.N. Goodier, in: Theory of Elasticity (McGraw-Hill, New York, 1970) Ch. 4.
- [7] D.W. Hairston and C.R. Frye, Evaluation of Tube Deposits Oconee 2A OTSG Metallurgy Sample Number 244, Duke Power Co. memo to R.W. Eaker, May 14, 1985.
- [8] Z. Szlarska-Smialowska, in: Splitting Corrosion of Metals (NACE, 1986).